

¹⁴V. G. Gorshkov and V. S. Polikanov, Pis'ma Zh. Eksp. Teor. Fiz. **9**, 464 (1969) [JETP Lett. **9**, 279 (1969)].
¹⁵C. Fronsdal, Phys. Rev. **179**, 1513 (1969).
¹⁶V. G. Gorshkov, A. I. Mikhailov, and V. S. Polikanov, Nucl. Phys. **55**, 273 (1964).
¹⁷V. G. Gorshkov and S. G. Sherman, Pis'ma Zh. Eksp. Teor. Fiz. **17**, 519 (1973) [JETP Lett. **17**, 374 (1973)].
¹⁸E. G. Drukarev, V. G. Gorshkov, A. I. Mikhailov, and S. G. Sherman, Phys. Lett. A **46**, 467 (1974).
¹⁹A. W. Adler and S. G. Cohen, Phys. Rev. **146**, 1001 (1966).
²⁰W. K. Roberts and D. C. Liu, Bull. Amer. Phys. Soc. **11**, 368 (1966).

²¹G. Jarlskog, L. Jonsson, S. Prunster, H. D. Shulz, H. J. Willutzki, and G. G. Winter, Phys. Rev. D **8**, 3813 (1973).
²²R. M. Dzhilkibaev, É. A. Kuraev, V. A. Khoze, and V. S. Fadin, Yad. Fiz. **19**, 699 (1974) [Sov. J. Nucl. Phys. **19**, 353 (1974)].
²³P. A. Franken, A. E. Hill, C. W. Peters, and G. Weinreich, Phys. Rev. **7**, 116 (1961).
²⁴F. Mandl and T. H. R. Sjöyrmé, Proc. Phys. Soc. London Sect. A **219**, 497 (1952).
²⁵K. Kajantie and P. Lindblom, Phys. Rev. **175**, 2203 (1968).

Translated by J. G. Adashko

Theoretical pulse shapes for the photon (light) echo

S. O. Elyutin, S. M. Zakharov, and É. A. Manykin

Engineering-Physics Institute, Moscow

(Submitted 5 July 1978)

Zh. Eksp. Teor. Fiz. **76**, 835-845 (March 1979)

It is shown that the photon-echo pulse shape is governed both by the inhomogeneous broadening of the resonance level and by the parameters of the pump pulses. Short pulses of a strong external field produce a coherent echo response whose shape is wholly determined by inhomogeneous broadening. If the field is weak and the length of the first pulse is large in comparison with T_2^* , the profile of the echo is determined by the amplitude and shape of the pump pulses. In particular, if the "area" under the first pulse is less than $\pi/2$, there is a correlation between the shape of the first pulse and the echo. The results are then generalized to the case of approximate resonance.

PACS numbers: 42.65.Gv

1. INTRODUCTION

Photon (light) echo is beginning to be widely used as a method of studying kinetic phenomena in solids and gases. It is well known that photon echo (PE) was originally discovered¹ in ruby as far back as 1964 and has since been used in this crystal to investigate relaxation processes in the case of the hyperfine interactions between chromium ions and the nuclei of aluminum atoms.²⁻⁴ The range of materials in which the photon echo phenomenon has been observed and investigated has expanded considerably in recent years. In solids, the PE effect has been discovered, apart from $\text{Cr}^{3+}:\text{Al}_2\text{O}_3$ (Ref. 1), in $\text{Pr}^{3+}:\text{LaF}_3$ (Ref. 5), $\text{Nd}^{3+}:\text{CaWO}_4$ (Ref. 6), $\text{Nd}^{3+}:\text{YAG}$ (Ref. 7), and so on. It has also been seen in certain organic crystals.^{8,9} In gases, the PE effect has been investigated in SF_6 (Ref. 10), NH_2D (Ref. 11), C^{13}H_3 (Ref. 12), and SiF_4 (Ref. 13).

In most of these papers, the photon echo effect was used to determine the decay time T_2 of the PE signal, and this was then used as a source of information on the mechanism responsible for interatomic and intermolecular interactions. It is, however, important to emphasize that these characteristics are deduced from the PE pulse shape which, in general, is determined not only by the parameters of the medium (homogeneous and inhomogeneous broadening of the resonance level) but also by the shape, amplitude, and length of the

pump pulses. In many cases (especially in the case of short intervals between the pump pulses), it has not been possible to establish whether the PE signal shape is, in the final analysis, determined by the resonance medium or by the envelope of the pump pulses. The solution of this problem is important not only from the point of view of determining the relaxation characteristics of the material under investigation from PE data, but also for establishing the possibility of using PE as a means of storage and subsequent reconstitution of the time structure of pump pulses.

In this paper, we develop a theory of the photon-echo pulse shape and establish criteria for the utilization of the PE effect either as a method of obtaining T_2 and T_2^* or as a method of recording, storage, and reconstitution of the envelope of the first pump pulse. A numerical experiment was used to investigate violations of these criteria, and the envelope of the PE signal under more complicated conditions was investigated.

2. BASIC ASSUMPTIONS AND INITIAL RELATIONSHIPS

The production of pulses of coherent radiation is investigated in this paper under a number of assumptions.

1. The pump pulses are plane waves propagating in the z direction with phase velocity v in a medium with constant refractive index. The slow field and polariza-

tion envelopes in the moving frame are then given by the following equation¹⁴

$$\frac{\partial}{\partial z} \mathcal{E} \left(t - \frac{z}{v} \right) = -i \frac{2\pi\omega}{v} N_0 \left\langle p \left(t - \frac{z}{v} \right) \right\rangle, \quad (1)$$

where N_0 is the concentration of the resonance particles and ω is the frequency of the oscillations.

2. The change in the shape of the transmitted pulse is neglected, i.e., it is assumed that the reaction of the medium to the external field is small. Since it is clear that, in this case, $|\partial \mathcal{E} / \partial z| L \ll \mathcal{E}_a$ (L is the length of the specimen and \mathcal{E}_a is the amplitude of the incident pulse on the boundary of the medium), and if we use the set of optical Bloch equations given below [see (10)], we can show that, as in the case of gaseous media,¹⁵ the "given-field approximation" can be used provided

$$k_0 L \ll 1, \quad (2)$$

where $k_0 = 4\pi^2 \omega d^2 N_0 T_2^* / \hbar v$ is the attenuation coefficient for a weak signal,¹⁴ d is the modulus of the reduced matrix element of the dipole transition, and T_2^* is the time of reversible polarization relaxation. The inequality given by (2) indicates that absorption within the length of the specimen is small.

3. The pump pulses propagate in the same direction. Space-locking conditions $\mathbf{k}_e = 2\mathbf{k}_2 - \mathbf{k}_1$ and the fact that the wave vectors of the pump pulses are equal ($\mathbf{k}_1 = \mathbf{k}_2 = \mathbf{k}$) then yield $\mathbf{k}_e = \mathbf{k}$, where \mathbf{k}_e is the wave vector of the photon echo.

4. The driving signals have initial phases $\phi_1 = \phi_2 = 0$ and there is no phase modulation (chirp effect) at entry into the medium.

We now write down the basic relationships used in this paper. Suppose that the origin of coordinates lies on the boundary of the medium and the first pulse reaches it at a time $t=0$. The second optical pulse reaches the boundary after a time T . The polarization produced in the medium at the time when the PE pulse is produced¹⁶ can be written in the following form:

$$P_e(z, t) = N_0 d f_e(\tau_e) \exp[i(k_e z - \omega t - \pi/2)], \quad (3)$$

$$\tau_e = t - k_e z / \omega - \delta_1 - \delta_2 - 2T.$$

where δ_1 and δ_2 are the pulse lengths and the function $f_e(\tau_e)$ governs the shape of the PE signal and is defined by

$$f_e(\tau_e) = \int_{-\infty}^{+\infty} dx g(x) F_e(x) \exp[-i\tau_e x \theta_1 / \delta_1], \quad (4)$$

where

$$x = (\omega - \omega_0') \frac{\delta_1}{\theta_1}, \quad \theta_{1,2} = \frac{d\mathcal{E}_{a1,2}}{\hbar} \int_0^{\delta_{1,2}} r_{1,2}(t) dt, \quad (5)$$

In these expressions, t_0 is the time at which the driving pulse is turned on, ω_0' is the eigenfrequency of the two-level system, and $r_{1,2}(t)$ describes the time dependence of the pump pulses. The response function $F_e(x)$ shows the extent to which radiators that are not in resonance with the external field contribute to the polarization. For rectangular pulses,^{16,17}

$$F_e(x) = \left[\frac{\sin(\theta_1(1+x^2)^{1/2})}{(1+x^2)^{1/2}} + 2i \frac{x}{1+x^2} \sin^2 \left(\frac{\theta_1}{2} (1+x^2)^{1/2} \right) \right] \times \frac{\sin^2[\theta_1/2(1+E_1^2 x^2/E_2^2)^{1/2}]}{1+E_1^2 x^2/E_2^2}, \quad (6)$$

$$E_{1,2} = d\mathcal{E}_{a1,2} T_2^* / \hbar. \quad (7)$$

We note that irreversible relaxation processes are not taken into account in (6).

The integral given by (4) will be evaluated in the course of derivation of (16)–(22) for the most frequently encountered Lorentzian and Gaussian distribution functions:

$$g(x) = \begin{cases} \frac{1}{\pi} \frac{E_1}{(1+E_1^2(x+\Delta)^2)} \\ \pi^{-1/2} E_1 \exp(-E_1^2(x+\Delta)^2) \end{cases}, \quad (8)$$

where

$$\Delta = (\omega - \omega_0) \delta_1 / \theta_1 = \Delta \omega \delta_1 / \theta_1. \quad (a)$$

3. STRONG FIELD ($E_1 \gg 1$)

We now suppose that the condition $E_1 \gg 1$ is satisfied for the first optical pulse, whereas, for the second pulse $E_2 \gg 1$ and the pulse is short, i.e., $\delta_2 \ll T_2^*$. In the strong field of the first pulse of length $\delta_1 < T_2^*$, the frequency spectrum of the transmitted signal exhibits an additional broadening $\sim E_1/T_2^*$, so that all the radiators are excited in an equivalent way within the linewidth. It is clear that the shape of the first pulse does not then affect the profile of the echo.

It is clear from (8) that the distribution function $g(x)$ depends parametrically on E_1 and decays much more rapidly than $F_e(x)$ in the case of a strong field. The main contribution to (4) is then due to the region $x \leq E_1^{-1}$. For small detuning Δ , the function given by (6) can be set equal to $F_e(0)$:

$$F_e(x) \approx F_e(0) = \sin \theta_1 \sin^2(\theta_2/2). \quad (9)$$

The method used to obtain the response function [Eq. (6)] used in the literature^{16,18,19} is not suitable for pulses of arbitrary shape. There is, however, another possible approach based on the solution of the set of Bloch-type equations¹⁴:

$$\begin{aligned} \dot{p} + \gamma p + ix\theta_1 p / \delta_1 + i n d^2 \mathcal{E}_a r(t) / \hbar &= 0, \\ \dot{n} - \frac{p-p^*}{2id} \frac{d\mathcal{E}_a}{\hbar} r(t) &= 0, \quad p(0) = 0, \quad n(0) = -1, \end{aligned} \quad (10)$$

where p is the slow polarization envelope, n is the inverted level population, and $\gamma = 1/T_2^*$.

The second and third terms in the first equation in (10) can be neglected in the strong field of the short first pulse. The expression for the polarization at the time corresponding to the onset of the echo is obtained from (10) by mating the solutions in the presence of the external field and in zero field. The final expression for the function representing the response of the medium to two strong pulses of arbitrary shape is

$$F_e(x) = -i \exp(-\gamma(\tau_e + 2T)) \sin \theta_1 \sin^2(\theta_2/2). \quad (11)$$

As expected, the strong-field response function corresponding to rectangular and arbitrary pulses is the same to within the exponential factor in (11), which describes the irreversible relaxation process.

The time structure of the polarization of the photon echo is determined by the integral in (4). If we use (9) and (11), we obtain the following two expressions, respectively:

$$f_e(\tau_e) = \begin{cases} \sin \theta_1 \sin^2(\theta_2/2) \exp(i\Delta\omega\tau_e - |\tau_e/T_2^*|) \\ \sin \theta_1 \sin^2(\theta_2/2) \exp(i\Delta\omega\tau_e - \tau_e^2/4T_2^{*2}) \end{cases} \quad (12)$$

and

$$f_e(\tau_e) = \begin{cases} \sin \theta_1 \sin^2 \frac{\theta_2}{2} \exp\left(i\Delta\tau_e \frac{\theta_1}{\delta_1} - \left|\frac{\tau_e \theta_1}{\delta_1 E_1}\right| - \gamma(\tau_e + 2T) - \frac{\pi}{2}\right) \\ \sin \theta_1 \sin^2 \frac{\theta_2}{2} \exp\left(i\Delta\tau_e \frac{\theta_1}{\delta_1} - \frac{\tau_e^2 \theta_1^2}{4\delta_1^2 E_1^2} - \gamma(\tau_e + 2T) - \frac{\pi}{2}\right) \end{cases} \quad (13)$$

Hence, it is clear that, in strong fields, pulses of arbitrary shape, and with frequency departing from the line center, produce a coherent response at the central frequency. The PE envelope is unrelated to the shape of the first pulse, and is determined exclusively by the frequency distribution function of the radiators.

4. WEAK FIELD ($E_1 \ll 1$)

We now suppose that the first exciting pulse is weak ($E_1 \ll 1$) and the second is strong and short, as in Sec. 3. The dependence of the distribution function on E_1 then leads to a relatively slow reduction in $g(x)$ for large x . This enables us to construct $F_e(x)$ for $E_1 \ll 1$ by going to the limit of large x in (6). We thus obtain

$$F_e(x) = \frac{2}{x} \sin^2 \frac{\theta_1 x}{2} \sin^2 \frac{\theta_2}{2} \exp\left(\frac{ix\theta_1}{2}\right). \quad (14)$$

This expression is not, in general, correct for $x < 1$ in (4), but the additional requirement $\theta_1 < 1$ ensures that the response function given by (9), which is valid for $x < 1$, agrees with (14) in this region and is proportional to b_1 . The expression given by (14) can therefore be used throughout the range of integration in (4).

If we now suppose that the first pulse can have an arbitrary shape, the response function can be obtained from (10) in which the inverted population is assumed to be constant: $n = n(0) = -1$. Without going into detail, we simply reproduce the final result:

$$F_e(x) = \frac{E_1 \sin^2(\theta_2/2) \exp[-\gamma(\tau_e + 2T)]}{2^{\frac{1}{2}} T_2^*} \int_{-\infty}^{+\infty} \frac{R^*(\nu) \exp(-i\nu\delta_1)}{\nu + \theta_1 x / \delta_1 + i\gamma} d\nu, \quad (15)$$

where $R(\nu)$ is the Fourier transform of the external field.

It is not difficult to see that, in the special case of a rectangular first pulse, the expression given by (15) becomes identical with (14), apart from the exponential factor. We can therefore use these two expressions to evaluate $f_e(\tau_e)$ for both rectangular and arbitrary pulses.

Substitution of (14) in (4) yields

$$f_e(\tau_e) = iE_1 \sin^2(\theta_2/2) \exp(i\Delta\omega\tau_e) \left[\exp(-i\Delta\omega\delta_1 - (\tau_e - \delta_1)^2/4T_2^{*2}) \times Z(\Delta\omega T_2^* + i(\tau_e - \delta_1)/2T_2^*) - \exp(-\tau_e^2/4T_2^{*2}) Z(\Delta\omega T_2^* + i\tau_e/2T_2^*) \right], \quad (16)$$

where

$$Z(\xi) = \pi^{-1/2} \int_{-\infty}^{+\infty} \frac{dz e^{-z^2}}{z - \xi}$$

is the plasma function.²⁰ Similarly,

$$f_e(\tau_e) = \begin{cases} iE_1 \sin^2 \frac{\theta_2}{2} \exp\left[-\frac{\tau_e}{T_2^*} + i\Delta\omega(\tau_e - \delta_1)\right] \frac{1 - \exp(\delta_1/T_2^*)}{i + \Delta\omega T_2^*}, & \tau_e < 0, \\ iE_1 \sin^2 \frac{\theta_2}{2} \exp\left[\frac{\tau_e}{T_2^*} + i\Delta\omega(\tau_e - \delta_1)\right] \frac{\exp(-\delta_1/T_2^*) - 1}{i - \Delta\omega T_2^*}, & \tau_e > \delta_1, \\ iE_1 \exp[i\Delta\omega(\tau_e - \delta_1)] \sin^2 \frac{\theta_2}{2} \left[\frac{\exp[(\tau_e - \delta_1)/T_2^*]}{i - \Delta\omega T_2^*} + \frac{\exp(-\tau_e/T_2^*)}{i + \Delta\omega T_2^*} \right] - \frac{2E_1 \sin^2(\theta_2/2)}{1 + \Delta\omega T_2^*}, & 0 < \tau_e < \delta_1. \end{cases} \quad (17)$$

Expressions (16) and (17) correspond to the Gaussian and Lorentzian distribution functions, respectively. In precisely the same way, substitution of the response function (15) in (4) yields:

$$f_e(\tau_e) = \frac{E_1^2 \delta_1 \sin^2(\theta_2/2)}{2^{\frac{1}{2}} T_2^* \theta_1} \exp\left[i\frac{\tau_e \theta_1 \Delta}{\delta_1} - \gamma(\tau_e + 2T) - \frac{\tau_e^2 \theta_1^2}{4E_1^2 \delta_1^2}\right] \int_{-\infty}^{+\infty} R^*(\nu) e^{-i\nu\delta_1} Z(\xi) d\nu, \quad (18)$$

where

$$\xi = i\frac{\tau_e \theta_1}{2E_1 \delta_1} + E_1 \Delta - i\gamma \frac{\delta_1 E_1}{\theta_1} - \nu \frac{\delta_1 E_1}{\theta_1}.$$

It is interesting to note that, in particular, (16) and (17) yield the law describing the decay of the amplitude with increasing $\Delta\omega$, which is determined by the form of the distribution function. For example, if we use (14) and the properties of the plasma function (20), we can show that $f_e(\tau_e) \sim \exp(-\Delta\omega^2 T_2^{*2})$.

We emphasize that the departure from resonance leads to an additional broadening of the spectrum of the echo signal. In particular, when $\delta_1 \gg T_2^*$, the first term can be neglected for $0 < \tau_e < \delta_1$. This is clear, for example, from (17). This, in turn, leads to the fact that the central part of the PE pulse is generated at the incident field frequency and is constant in amplitude, whereas the leading and trailing edges fall exponentially and their frequencies are shifted toward the line center. The wave vector is, of course, also incremented by $\sim \Delta\omega/\nu$.

In the region of exact resonance, the shape of the coherent response as $\Delta\omega \rightarrow 0$ is much clearer. In the limit of $\Delta\omega = 0$, we obtain the following two expressions from (16) and (17), respectively:

$$f_e(\tau_e) = -\pi^{1/2} E_1 \sin^2 \frac{\theta_2}{2} \left[\operatorname{erf}\left(\frac{\tau_e}{2T_2^*}\right) - \operatorname{erf}\left(\frac{\tau_e - \delta_1}{2T_2^*}\right) \right], \quad (19)$$

$$f_e(\tau_e) = \begin{cases} E_1 \sin^2 \frac{\theta_2}{2} \exp\left(-\frac{\tau_e}{T_2^*}\right) \left[1 - \exp\left(\frac{\delta_1}{T_2^*}\right) \right], & \tau_e > \delta_1, \\ E_1 \sin^2 \frac{\theta_2}{2} \exp\left(\frac{\tau_e}{T_2^*}\right) \left[\exp\left(-\frac{\delta_1}{T_2^*}\right) - 1 \right], & \tau_e < 0, \\ E_1 \sin^2 \frac{\theta_2}{2} \left[\exp\left[\frac{(\tau_e - \delta_1)}{T_2^*}\right] + \exp\left(-\frac{\tau_e}{T_2^*}\right) \right] - 2E_1 \sin^2 \frac{\theta_2}{2}, & 0 < \tau_e < \delta_1. \end{cases} \quad (20)$$

These two expressions also show that the time of appearance of the photon echo is delayed by $\delta_1/2$.

Physically, $\theta_1 < 1$ and $\delta_1 \gg T_2^*$ mean that, in effect, only a narrow part of the line near the frequency of the

incident radiation is excited. This enables us to assume that the distribution of radiators over the spectrum of the first pulse can be represented by a constant.²¹ The distribution $g(x)$ can then be taken outside the integral sign in (4) at $x=0$. The integral in (4) can then be evaluated for the response functions (14) and (15) and the result is

$$f_e(\tau_e) = -2\pi i g(0) \sin^2(\theta_2/2) [\eta(\tau_e - \delta_1) - \eta(\tau_e)], \quad (21)$$

where $\eta(t)$ is the unit function and

$$f_e(\tau_e) = 2^{3/2} \pi^{1/2} \frac{g(0)}{T_2^*} \frac{E_1 \delta_1}{\theta_1} \sin^2 \frac{\theta_2}{2} \exp[-2\gamma(\tau_e + T)] r_1(\delta_1 - \tau_e). \quad (22)$$

It is clear from (21) and (22) that the shape of the first pulse is completely reproduced as if it were reflected at the point $\delta_1 + \delta_2 + T$ on the time axis. Naturally, the echo appears at the same time as before, and is shifted by $\delta_1/2$ toward large times.

For completeness, we reproduce the expressions describing the field and the PE intensity:

$$\mathcal{E}_e(z, t) = \frac{\hbar k_0 z}{2i\pi^{1/2} d T_2^*} f_e(\tau_e) \exp[i(k_0 z - \omega t)], \quad (23)$$

$$I_e(z, t) = \frac{v \hbar^2 (k_0 z)^2}{32\pi^2 d^2 T_2^{*2}} |f_e(\tau_e)|^2. \quad (24)$$

5. NUMERICAL RESULTS

The above analytic expressions refer to the limiting cases of strong and weak fields corresponding to the first pulse, and strong and short second pulse. However, in intermediate fields,^{18, 22, 23} an analytic solution is hardly possible. We therefore resorted to numerical methods to solve the basic set of equations (10) to an absolute precision of the order of 10^{-3} . The first two light pulses (Figs. 1 and 2), taken in units of \hbar/dT_2^* , were specified as the boundary conditions for the numerical procedure, and the third pulse (the PE signal) was the computed function $f_e(\tau)$. The pump pulses and the echo are shown on the same scale for convenience, although there is a connection between \mathcal{E}_e and f_e [see (23)]. The time $\tau = (t - z/v)/T_2^*$ is plotted along the hor-

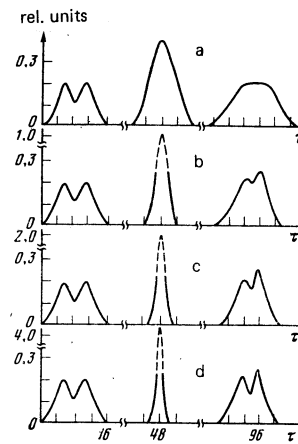


FIG. 2. Appearance of correlation between the shape of the first pulse and the echo profile as the second pulse amplitude E_2 increases: a) 0.4, b) 1.0, c) 2.0, d) 4.0; $\theta_1 = \pi/2$, $\theta_2 = \pi$.

izontal axis. The results refer to exact resonance and the Gaussian line shape.

Let us now suppose that the pump pulses are such that $\theta_1 > \pi$ and $\theta_2 > \pi$. The PE profile then depends on the amplitude E_1 of the first pulse. When $E_1 > 1$ or $\delta_1 < T_2^*$, the pulse has a broad spectrum and excites the entire line in an equivalent fashion. By analogy with (12), the shape of the coherent response then corresponds to the profile of an inhomogeneously broadened line (Fig. 1c). The situation becomes substantially more complicated if the amplitude of the first pulse begins to decrease. In this situation, $E_1 < 1$ and $x > 1$, and the angles of rotation of the pseudodipole moments $\varphi_x = \theta_1(1+x^2)^{1/2}$ will be different for different x and, in particular, may be greater than π . The phasing of the radiators then occurs in different "planes," as in the superradiance delay effects.¹⁶ This complicated process of radiator phase locking naturally leads to the multihump structure (Fig. 1b).^{18, 23} The shape of the PE pulse may not then be related to the time structure of the first pulse (Figs. 1b and d).

It follows from (16), (17), (21), and (22) that the correlation between the shape of the first pulse and the photon-echo signal will occur if $\theta_1 < 1$ and $\delta_1 \gg T_2^*$. It turns out that the envelope of the response is a mirror reflection of the polarization profile induced by the first signal and, therefore, the increase in the PE amplitude with time (Fig. 1a) is essentially a reproduction of the relaxation of the polarization produced by the first pulse.

It is well known that the application of a strong ($E_2 > 1$) and short ($\delta_2 < T_2^*$) second pulse is analogous to time reversal, and this is the reason for the radiator phase locking at the time of appearance of the echo. The second-pulse parameters which we have just quoted are also the necessary condition for a correlation between the shape of the first pulse and the PE (Figs. 2b-d). In the opposite case ($E_2 \leq 1$), the effect of the time structure of the first pulse on the echo signal is reduced (Fig. 2a).

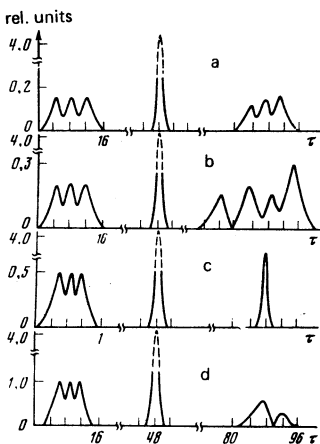


FIG. 1. Echo pulse shape under different excitation conditions: a) $\theta_1 = \pi/2$; $E_1 = 0.2$; $\theta_2 = \pi$; $E_2 = 4.0$ - echo profile repeats the pulse shape; b) $\theta_1 = 3\pi/2$; $E_1 = 0.2$ - multihump echo; c) $\delta_1 < T_2^*$; $E_1 = 0.5$ - echo reproduces the line shape; d) $\theta_1 = 3\pi/2$; $E_1 = 1.0$ - double-hump echo.

6. COMPARISON WITH EXPERIMENT

We have already noted that the high sensitivity of the PE method to the kinetics of fast relaxation processes has stimulated experimental studies of echo signals in a broad range of materials. Several experimental papers^{2,3,6} have appeared in recent years on the "anomalous" light echo. This echo is unusual in that this coherent response has a complicated but well-defined time profile. One of the first papers in this field was by Liao and Hartmann,³ who reported the observation of a two-hump echo in ruby. Estimates of θ_1 based on the parameters reported by Liao and Hartmann,³ show that $\theta_1 = 10$. When this is assumed, calculations performed for rectangular pump pulses²³ are found to reproduce the two-hump structure of the echo response reported by Liao and Hartmann.³ A similar phenomenon is possible in gases.¹⁷

A detailed experimental study of the anomalous echo has been performed in the case of $\text{Nd}^{3+}:\text{CaWO}_4$ by Samartsev *et al.*^{2,6} For example, they observed the anomalous light echo in ruby² but, in contrast to Liao and Hartmann,³ they used incident pulses of complicated shape with pulse length of the order of 7–10 nsec.

The quantities E_1 and E_2 [see (7)] in the experiments of Samartsev *et al.*² were 0.2 and 0.4, respectively. The pulse area was therefore $\theta_1 \sim 20$. Curve c in Fig. 3 shows oscillogram traces of the light echo reported by Samartsev *et al.*,² whereas curve d was calculated for conditions similar to those used in the experiment. It is clear that the reasons for the appearance of the anomalous echo are the same as in the work of Liao and Hartmann.³ It is interesting to note that several experimenters^{4,2,6} have recorded a delay in the appearance of the PE, and there has been a recent report²⁴ of the detection of coherent response at time prior to $\tau_e = 0$.

Figure 4 shows that, when the area θ_1 is changed from $\pi/4$ to $7\pi/4$, the position of the echo maximum on the time scale does not have a monotonic behavior near $\tau_e = 0$, but exhibits oscillations about the average value of $\tau_e = 0$. Hence, when the area of the first pulse is

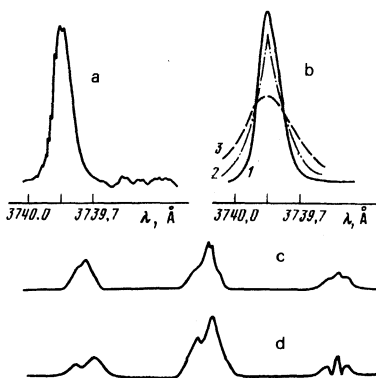


FIG. 3. Experimental data for molecular crystals⁸ (a) and calculated profile of inhomogeneously broadened line (b). The figure also shows the echo response of the medium to two-pulse excitation: c—measured,² d—calculated from (10). The echo pulse is the first on the right.

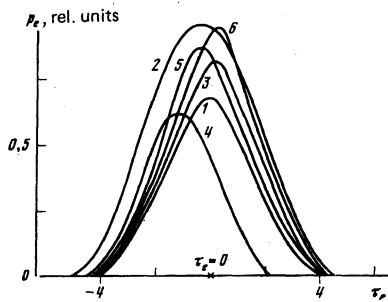


FIG. 4. Shift in the position of the echo toward the region $\tau_e < 0$. The values of θ_1 for curves 1–6 are $\pi/4$, $\pi/2$, $5\pi/4$, $3\pi/2$, and $7\pi/4$, respectively. Parameter values: $\delta_1 = 0.5T_2^*$, $\delta_2 = 0.5T_2^*$; $\delta_2 = \pi$, $E_2 = 4.0$.

varied, the echo signal may be either retarded or advanced in time. The reasons for this are still not clear and require further investigation.

New applications of the PE effect in ultrahigh-resolution spectroscopy have been reported as a result of experiments on coherent response in molecular crystals.^{8,9} Thus, Aartsma and Wiersma⁸ have measured the PE intensity as a function of the frequency of the incident light near resonance. They found that $I_e(\omega)$ had the Gaussian shape and, apparently, described the shape of an inhomogeneously broadened line. If it is assumed that this experiment was performed for $\theta_1 \lesssim 1$, it turns out that $E_1 < 10^{-2}$ and $\delta_1 \sim 100T_2^*$. It was shown earlier [see (21) and (22)] that, under these conditions, $I_e \sim g^2(0)$. The shape of the I_e curve corresponding to a detuning $\Delta\omega$ is thus found to be connected with the shape of the inhomogeneously broadened line.

Figure 3b shows the result of a numerical evaluation of the integral in (4) as a function of $\Delta\omega$. The $I_{e \max}(\Delta\omega)$ on the position of the maximum (Fig. 3a), and the area under the curve is normalized. The graphs shown in Fig. 3b were obtained by evaluating (4) with Gaussian (curve 1) and Lorentzian (curve 2) distribution functions. As can be seen, there is relatively good agreement with experimental data. It is interesting to note that the same calculation performed with $E_1 > 1$ and $\delta_1 < T_2^*$ yields, as expected, a linewidth that is greater than the experimental result (Fig. 3b, curve 3).

7. CONCLUSIONS

The shape of the PE envelope is thus found to depend on a number of conditions restricting the parameters of the pump pulses. Above all, it is important to emphasize that the influence of the shape of an inhomogeneously broadened line on the time evolution of the PE signal can, in general, be investigated only in the given-field approximation ($k_0 L < 1$). In dense resonance media,¹⁶ the echo profile may be distorted by the appearance of additional pulses of nutational origin and by multiple PE. The most effective utilization of the PE phenomenon as a method of determining the time of irreversible polarization relaxation (T_2) corresponds to the strong ($\mathcal{E}_1 > \hbar/dT_2^*$) and short ($\delta_1 < T_2^*$) pulses. The envelope of the PE signal under this type of excitation is found to depend only on the radiator frequency distri-

bution function and is not related to the profile of the first pulse. In the case of a strong pulse, the length of the echo signal can, of course, be used as a source of information on the half-width T_2^{*-1} of the inhomogeneously broadened line. Partial or complete reproduction by the PE profile of the shape of the first pulse will occur in the opposite situation in the case of an essentially nonequivalent excitation of the line when $\theta_1 < 1$ and $\delta_1 \gg T_2^*$, i.e., in the case of a weak field ($\mathcal{E}_1 < \hbar/dT_2^*$) first pulse.

It is interesting to note that, with this choice of parameters, we have the possibility of being able to investigate the shape of the inhomogeneously broadened line itself.

¹N. A. Kurnit, I. D. Abella, and S. R. Hartmann, *Phys. Rev. Lett.* **13**, 567 (1964).

²U. Kh. Kopvillem, V. R. Nagibarov, V. A. Pirozhkov, V. V. Samartsev, and R. G. Usmapov, *Pis'ma Zh. Eksp. Teor. Fiz.* **20**, 139 (1974) [*JETP Lett.* **20**, 60 (1974)].

³P. L. Liao and S. R. Hartmann, *Phys. Lett. A* **44**, 361 (1973).

⁴S. Meth and S. R. Hartmann, *Phys. Lett. A* **58**, 192 (1976).

⁵N. Takeuchi and A. Szabo, *Phys. Lett. A* **50**, 361 (1974).

⁶V. V. Samartsev, R. G. Usmanov, and I. Kh. Khodyev, *Pis'ma Zh. Eksp. Teor. Fiz.* **22**, 32 (1975) [*JETP Lett.* **22**, 14 (1975)].

⁷N. Takeuchi, S. Chandra, Y. C. Chen, and S. R. Hartmann, *Phys. Lett. A* **46**, 97 (1973).

⁸T. J. Aartsma and D. A. Wiersma, *Phys. Lett.* **36**, 1360 (1976).

⁹J. B. W. Morsink, T. J. Aartsma, D. A. Wiersma, and Y. C.

Chen, *Phys. Lett.* **49**, 34 (1976).

¹⁰J. R. Meckley and C. V. Heer, *Phys. Lett. A* **46**, 531 (1973).

¹¹L. Shoemaker and F. A. Hopf, *Phys. Rev. Lett.* **33**, 1527 (1974).

¹²J. Schmidt, P. R. Berman, and R. G. Brewer, *Phys. Rev. Lett.* **31**, 1103 (1973).

¹³R. J. Nordstrom, W. M. Gutman, and C. V. Heer, *Phys. Rev. Lett. A* **50**, 25 (1974).

¹⁴S. M. Zakharov and É. A. Manykin, *Pis'ma Zh. Eksp. Teor. Fiz.* **17**, 431 (1973) [*JETP Lett.* **17**, 308 (1973)].

¹⁵A. I. Alekseev and I. V. Evseev, *Zh. Eksp. Teor. Fiz.* **56**, 2118 (1969) [*Sov. Phys. JETP* **29**, 1139 (1969)].

¹⁶S. M. Zakharov and É. A. Manykin, *Kvantovaya Elektron. (Moscow)* **2**, 31 (1973) [*Sov. J. Quantum Electron.* **3**, 104 (1973)].

¹⁷A. I. Alekseev and I. V. Evseev, *Zh. Eksp. Teor. Fiz.* **68**, 456 (1975) [*Sov. Phys. JETP* **41**, 222 (1975)].

¹⁸N. Takeuchi, *IEEE J. Quantum Electron.* **QE-11**, 230 (1975).

¹⁹S. M. Zakharov, É. A. Manykin, and E. V. Onishchenko, *Zh. Eksp. Teor. Fiz.* **59**, 1307 (1970) [*Sov. Phys. JETP* **32**, 714 (1971)].

²⁰B. O. Fried and S. D. Conte, *The Plasma Function*, Academic Press, New York, 1961.

²¹S. Fernbach and W. G. Proctor, *J. Appl. Phys.* **26**, 170 (1955).

²²S. O. Elyutin, S. M. Zakharov, and É. A. Manykin, *Opt. Spektrosk.* **42**, 1005 (1977) [*Opt. Spectrosc. (USSR)* **42**, 581 (1977)].

²³S. O. Elyutin, S. M. Zakharov, and É. A. Manykin, *Kvantovaya Elektron. (Moscow)* **3**, 357 (1976) [*Sov. J. Quantum Electron.* **3**, 189 (1976)].

²⁴V. V. Smartsev, R. G. Usmanov, G. M. Ershov, and B. Sh. Khamidullin, *Zh. Eksp. Teor. Fiz.* **74**, 1979 (1978) [*Sov. Phys. JETP* **47**, 1030 (1978)].

Translated by S. Chomet

Effects of negative-ion formation and post-collision interaction in collisions between magnesium atoms and electrons

O. B. Shpenik, I. P. Zapesochnyi, E. É. Kontrosh, É. I. Nepiřpov, N. I. Romanyuk, and V. V. Sovter

Uzhgorod State University

(Submitted 6 July 1978)

Zh. Eksp. Teor. Fiz. **76**, 846-855 (March 1979)

Results are presented of investigations of the excitation of magnesium atoms by monoenergetic electrons from the excitation threshold to 11 eV. The structure of the optical excitation functions is investigated in detail both up to and above the ionization threshold. It is established that the structure of the excitation functions up to the ionization threshold is governed by the decay of the short-lived states of the negative magnesium ion, while above the ionization threshold it is governed by the post-collision interaction of the emitted and scattered electrons. Possible negative-ion states and auto-ionization levels of the magnesium atoms, which lead to singularities of the excitation functions of the spectral lines, are discussed.

PACS numbers: 34.80.Dp

INTRODUCTION

Experiments aimed at studying the excitation of atoms of alkaline-earth elements by electron impact have recently been performed.^{1,2} The effective cross sections

for the excitation of spectral transitions and energy levels were determined, and some singularities of the excitation of the lower levels of these atoms were revealed. To obtain a more detailed and complete information for atomic physics, precision investigations of